

ANALYSIS OF THE INTEGRATED INTENSITY OF THE CENTRAL PEAKS CALCULATED AS A FUNCTION OF TEMPERATURE IN THE FERROELECTRIC PHASE OF LITHIUM TANTALATE

by

Ali KIRACI^{a*} and Hamit YURTSEVEN^b

^a Inter-Curricular Courses Department, Cankaya University, Ankara, Turkey

^b Department of Physics, Middle East Technical University, Ankara, Turkey

Original scientific paper

<https://doi.org/10.2298/TSCI170614289K>

The integrated intensity of the central peak is calculated as a function of temperature in the ferroelectric phase ($T < T_C$) of nearly stoichiometric LiTaO_3 . This calculation is performed using the temperature dependence of the order parameter obtained from the mean field theory at temperatures lower than the transition temperature T_C ($T_C = 963 \text{ K}$) of this crystal. The calculated values of the order parameter (squared) are fitted to the integrated intensity of the central peaks as observed from the Raman and Brillouin scattering experiments as reported in the literature in the ferroelectric phase of nearly stoichiometric LiTaO_3 . Our results are in good agreement with the observed behavior of LiTaO_3 crystal. Because of the applications of LiTaO_3 in several academic disciplines including the material science and thermal science, it is beneficial to investigate dynamic properties of this crystal such as the damping constant, inverse relaxation time and the activation energy as also we studied here.

Key words: *integrated intensity, order parameter, damping constant, relaxation time, LiTaO_3*

Introduction

Lithium tantalate (LT) with the perovskite structure exhibits ferroelectricity and pyroelectricity. Due to its high mechanical stability and low thermal expansion properties, LT is widely used in non-linear optical and electro optical applications [1, 2]. As a pyroelectric detector, LT is a powerful candidate for determining particle energy and absolute flux in supersonic molecular beams of gases [3]. It has been reported the efficient role of this crystal for temperature sensing in adsorption microcalorimetry [4]. The LaTiO_3 has a high Curie temperature that allows for higher temperature studies. The phase transition temperature of this material depends on the mol ratio of $[\text{Li}_2\text{O}]:[\text{Ta}_2\text{O}_5]$. As a ferroelectric material, LT of the congruent composition, $[\text{Li}_2\text{O}]:[\text{Ta}_2\text{O}_5] = 48.5:51.5$ (mol %), undergoes a ferroelectric phase transition at about $T_C = 873 \text{ K}$ [5]. It is rhombohedral with the space group $R3c$ (C_{3v}^6) below T_C and it is rhombohedral with the space group $R\bar{3}c$ (D_{3d}^6) above T_C [6].

A number of experimental works including Raman [7, 8], hyper-Raman [7], quasi-elastic light scattering [9], studies by using ultrasonic phase comparison method [10], and on its dielectric properties [11] have been reported in the literature to understand the mechanism

* Corresponding author, e-mail: akiraci@cankaya.edu.tr

of the phase transition in LT. Although very contradictory results have been declared, the lattice dynamics of LT crystals plays an important role in the phase transition mechanism. A soft mode with the $A_1(z)$ symmetry in the ferroelectric phase has been observed by Johnston and Kaminov [12]. From the infrared reflectivity measurement by Sevoin and Gervais [13], a soft mode has been detected in both ferroelectric and paraelectric phases of LT crystal. Moreover, the existence of the soft mode at room temperature has been reported by the terahertz time domain spectroscopy [14] and the impulsive stimulated Raman scattering [15, 16] measurements. On the contrary, the Raman scattering study by Raptis [17] and the investigation of the pressure dependent Raman spectra by Jayaraman and Ballman [18] showed no evidence for the mode softening. In their study Samuelsen and Grande [19], explained how the gradual ordering of Li atoms can be related to the temperature dependence of the spontaneous polarization. It has also been reported that in the paraelectric phase, Li ion took positions $+0.00337$ nm on either side of the oxygen plane with equal probability [20] which can indicate an order-disorder type phase transition. However, Tomeno and Matsumura [11] have noticed a large Curie constant ($1.43 \cdot 10^5$ K) which can describe a displaced type phase transition. Additional to the different experimental studies as previously stated, a very limited number of theoretical works have been carried out. For example, Penna *et al.* [21, 22] have explained the dynamic origin of the central peaks (CP) of LT that are associated with the phase transition mechanism in ferroelectric materials.

In this study, we calculate the temperature dependence of the Raman and Brillouin integrated intensities of CP of nearly stoichiometric LiTaO_3 (SLT) [Li_2O]:[Ta_2O_5] = 49.9: 50.1 (mol %) in the ferroelectric phase ($T_c = 963$ K). This calculation was performed by relating the observed intensity [7] with the order parameter calculated from the mean field theory [23]. As an extension of this work, we predicted the temperature dependence of the damping constant (linewidth) of the CP through the pseudospin-phonon coupled (PS) [24] and the energy fluctuation (EF) [25] models for both ferroelectric and paraelectric phases of SLT. Also, we calculated the inverse relaxation time, τ^{-1} , due to the ionic motion regarding the CP close to the transition temperature ($T_c = 963$ K) for SLT. Our calculated values of the inverse relaxation time using the predicted values of the order parameter (squared) by means of the PS and EF model, are compared with the experimental inverse relaxation time [7] through the fitting procedure close to the T_c for SLT. Finally, we extracted values of the activation energy of this ferroelectric SLT crystal in the temperature range studied.

Calculations and results

The mean field theory approach implies a monodomain state of crystal with the homogenous distribution of the polarization (order parameter) P . The temperature dependence of the integrated intensity of the CP of SLT can be calculated using the order parameter, P , derived from the mean field theory according to the relation [23]

$$\begin{aligned}
 & 1 - 2 \exp\left(\frac{-2T_c}{T}\right), \quad T \ll T_c \\
 P \approx & \sqrt{3\left(1 - \frac{T}{T_c}\right)}, \quad 0 < (T_c - T) < T_c \\
 & 0, \quad T_c < T
 \end{aligned} \tag{1}$$

We associated the order parameter (squared) with the temperature dependence of the integrated intensities of the CP in the ferroelectric phase of LiTaO_3 . On this basis, we fitted the calculated

values of the order parameter to the observed intensity (normalized) (I/I_{max}) from the Raman and Brillouin scattering experiments [7] for the CP at temperatures $T < T_C$ according to a linear equation:

$$I/I_{max} = a + bP^2 \quad (2)$$

where a and b are constants.

Table 1 gives the values of a and b within the temperature range indicated for the CP in LiTaO₃ for both Raman and Brillouin scattering data [7]. The temperature dependence of the integrated intensity of the CP which was calculated through eq. (1) in the ferroelectric phase of LiTaO₃ using both data [7], is given in figs. 1 and 2.

Table 1. Values of the fitting parameters through eq. (2) using the observed Raman and Brillouin integrated intensities of CP [7] in the ferroelectric phase ($T < T_C$) of SLT crystal ($T_C = 963$ K)

Integrated Intensity	a	$-b$	T [K]
Raman	0.35	0.34	$298 < T < 771$
	1.10	1.94	$824 < T < 946$
Brillouin	0.26	0.27	$562 < T < 873$
	1.27	4.24	$894 < T < 947$

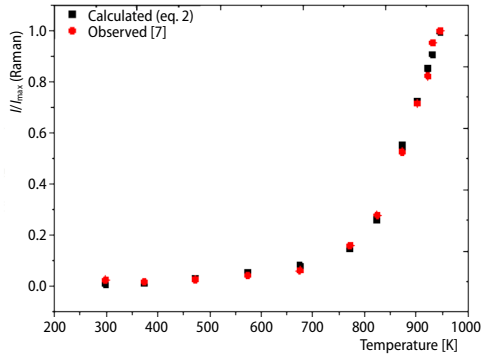


Figure 1. Temperature dependence of the normalized Raman integrated intensity I/I_{max} of the CP which was calculated by eq. (1) through eq. (2) in the ferroelectric phase of SLT ($T_C = 963$ K); the observed Raman data [7] of the integrated intensity are also shown here

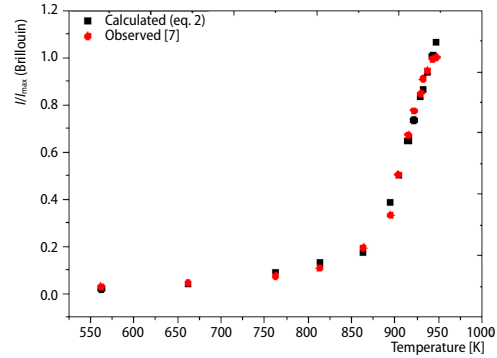


Figure 2. Temperature dependence of the normalized Brillouin integrated intensity I/I_{max} of the CP which was calculated by eq. (1) through eq. (2) in the ferroelectric phase of SLT ($T_C = 963$ K); the observed Brillouin data [7] of the integrated intensity are also shown here

As an extension of this work, we predicted the damping constant (linewidth), Γ , as a function temperature and we calculated the inverse relaxation time, τ^{-1} , due to the ionic motion regarding CP of LiTaO₃ close to the ferroelectric-paraelectric phase transition temperature $T_C = 963$ K. We used the pseudospin-phonon coupled model [24] and the EF model [25] to predict the temperature dependence of the damping constant of the CP for LaTiO₃ in both ferroelectric and paraelectric phases. The temperature dependence of the damping constant in the PS model [24]:

$$\Gamma = \Gamma_0 + A(1 - P^2) \ln \left[\frac{T_C}{T - T_C(1 - P^2)} \right] \quad (3)$$

where Γ_0 is the background bandwidth and A is a constant which we take as unity. Likewise, the temperature dependence of the damping constant due to EF model [25] can be expressed:

$$\Gamma = \Gamma_0 + A \sqrt{\frac{T(1-P^2)}{T-T_C(1-P^2)}} \quad (4)$$

where Γ_0 and A are constants as before. We consider that the integrated intensity, I , is proportional to the square of the order parameter:

$$P^2 \propto I, \quad T < T_C \quad (5)$$

in the ferroelectric phase, and for the paraelectric phase:

$$P^2 \propto 1 - I, \quad T > T_C \quad (6)$$

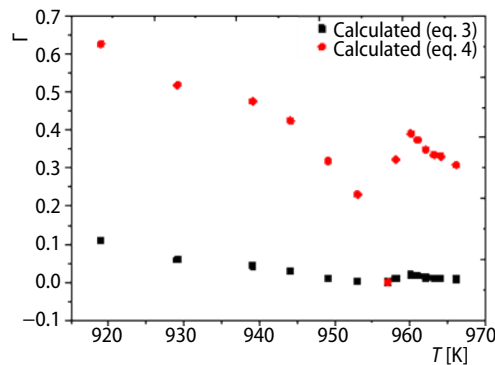


Figure 3. Calculated values of the damping constant from the PS model (eq. 3) and EF model (eq. 4) as a function of temperature for the CP of the SLT crystal close to the transition temperature $T_C = 963$ K

regarding CP as a function of temperature by considering the proportionality of the order parameter to the Raman integrated intensity through eqs. (5) and (6) in the ferroelectric and paraelectric phase of LiTaO_3 , respectively. Those calculated values of the inverse relaxation time values are related to the observed data [7] according to a quadratic equation given:

$$\tau_{\text{obs}}^{-1} = c_0 + c_1 \tau_{\text{cal}}^{-1} + c_2 (\tau_{\text{cal}}^{-1})^2 \quad (8)$$

The coefficients of eq. (8) are given in tab. 2. We plot our calculated values of the inverse relaxation time, eq. (7) as a function of temperature with the experimental data [7] in fig. 4.

Finally, the energy barrier between different orientations of the ion groups, namely the activation energy [26], can be calculated from the damping constant eqs. (3) and (4) by using the temperature dependence of the total linewidth [27, 28]:

$$\Gamma \cong \Gamma_{\text{vib}} + C \exp\left(\frac{-U}{k_B T}\right) \quad (9)$$

here k_B is the Boltzmann constant and C is a constant.

as the disorder parameter. We calculated the temperature dependence of the damping constant for the CP of LiTaO_3 using the observed data for the Raman integrated intensity [7]. We plot in fig. 3 the linewidths calculated from eqs. (3) and (4) of the CP as a function of temperature for the ferroelectric-paraelectric transition ($T_C = 963$ K) in LiTaO_3 .

The inverse relaxation time, τ^{-1} , due to the ionic motion regarding CP in LaTiO_3 can be calculated by using:

$$\tau^{-1} = \frac{P^2}{\Gamma} \quad (7)$$

where P is the order parameter and Γ is the damping constant. We calculated the inverse relaxation time, τ_{cal}^{-1} , due to the ionic motion re-

Table 2. Values of the coefficients obtained by fitting τ_{cal}^{-1} to the observed inverse relaxation time τ_{obs}^{-1} according to eq. (8) for the CP of SLT close to the transition temperature $T_C = 963$ K, τ_{cal}^{-1} values were calculated from eq. (7) using the damping constant Γ eqs. (3) and (4)

Γ	$c_0 \cdot 10^{11}$	c_1	$c_2(\text{s})$	T [K]
Eq. (3)	21.5	$2.54 \cdot 10^{10}$	$6.75 \cdot 10^7$	918 K-958
	9.16	$1.12 \cdot 10^9$	$5.40 \cdot 10^7$	961 K-966
Eq. (4)	4.15	$2.81 \cdot 10^{12}$	$5.10 \cdot 10^{12}$	918 K-958
	12.2	$5.57 \cdot 10^{12}$	$7.39 \cdot 10^{12}$	961 K-966

Since the vibrational relaxation, Γ_{vib} , is very small in the vicinity of T_C , it can be neglected. Therefore, the activation energy U can be calculated:

$$\ln \Gamma = \frac{-U}{k_B T} \quad (10)$$

The activation energy U of ions responsible for CP was calculated close to the transition temperature ($T_C = 963$ K) of the LiTaO₃ using eq. (10). The damping constants, Γ , calculated through eqs. (3) and (4) were used in eq. (10). Table 3 gives our calculated values of the activation energy in the temperature intervals indicated.

Discussion

The Raman and Brillouin integrated intensities were calculated for CP of nearly stoichiometric lithium tantalate as a function of temperature using the order parameter (squared) eq. (1) as given in figs. 1 and 2, respectively. This calculation was performed by means of the fitting procedure of the order parameter, P^2 , with the observed integrated intensity data [7] in the temperature ranges of $298 < T < 771$, $824 < T < 946$ for the Raman integrated intensity and $562 < T < 873$, $894 < T < 947$ for the Brillouin integrated intensity as given in tab. 1. Our calculated values of the Raman and Brillouin integrated intensities increase gradually well below the transition temperature ($T_C = 963$ K) and increase very rapidly toward this transition temperature and these intensities reached their maximum values in the vicinity of the T_C in the ferroelectric phase of SLT crystal also as observed experimentally [7]. It has been reported that CP is formed due to the temperature dependent dynamical fluctuations of the domains [21, 22]. Our calculation indicates that the CP of this SLT crystal plays an important role for the order-disorder phase transition at around T_C .

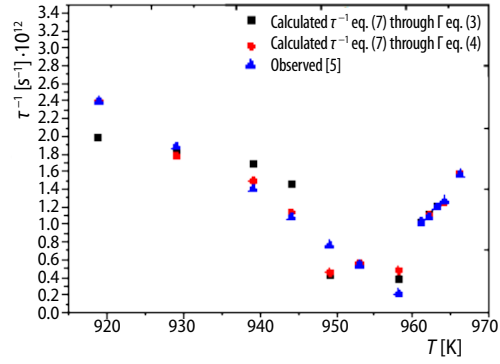


Figure 4. Temperature dependence of the inverse relaxation time τ^{-1} calculated from eq. (7) through the damping constant Γ eqs. (3) and (4) for the CP of SLT crystal ($T_C = 963$ K); experimental data [7] for the relaxation time are also shown here

Table 3. Values of the activation energy, U , according to eq. (10) where the damping constant calculated from eqs. (3) and (4), was used in both ferroelectric ($T < T_C$) and paraelectric ($T > T_C$) phases for the SLT crystal. $k_B T_C$ value is also 0.08 eV ($T_C = 963$ K)

Damping constant Γ	Activation energy $-U$ [eV]	Temperature range [K]
Eq. (3)	3.74	$918 < T < 944$
	7.24	$944 < T < 957$
	11.49	$961 < T < 966$
Eq. (4)	1.09	$918 < T < 944$
	1.88	$944 < T < 957$
	2.87	$961 < T < 966$

The temperature dependence of the damping constant (linewidth), Γ , due to the ionic motion regarding the CP in SLT crystal, was predicted using the PS model, eq. (3) and the EF model, eq. (4), below and above phase transition temperature ($T_C = 963$ K), as given in fig. 3. Our calculated values of the Raman integrated intensity were associated with the order parameter, P^2 , in the ferroelectric phase and with the disorder parameter $(1 - P^2)$ in the paraelectric phase of this crystal. We then considered the normalized Raman integrated intensity, I/I_{\max} , as an order parameter squared since P can take values between 0 and 1. Damping constant calculated from both models (PS and EF) decreased below T_C in the ferroelectric phase and it increased above T_C in the paraelectric phase.

The inverse relaxation time τ^{-1} , eq. (7) was evaluated by using our calculated values of the Raman integrated intensity through eq. (2) and using the calculated values of the damping constant from both models (PS and EF) through eqs. (3) and (4). Those calculated values of the inverse relaxation time were then fitted to the observed data [7] according to eq. (8) in the temperature ranges of $918 < T < 958$ and $961 < T < 966$, with the fitting parameters, tab. 2, as given in fig. 4. The calculated values of the inverse relaxation time τ^{-1} , eq. (7) through the EF model, eq. (4), agree better than those calculated through the PS-CP model, eq. (3) both in the ferroelectric and paraelectric phases of SLT crystal.

Finally, we deduced values of the activation energy for this crystal through eq. (10) in the temperature intervals indicated, with the $k_B T_C$ value, tab. 3. Negative values of the activation energy indicate that the energy of the SLT crystal decreases below and above the transition temperature ($T_C = 963$ K).

Conclusions

The Raman and Brillouin integrated intensities of the CP of nearly SLT were calculated at various temperatures in the ferroelectric phase by using the mean field theory. This calculation was performed by means of the order parameter (squared) associated with the Raman and Brillouin integrated intensities of the CP in SLT. Our calculated values agree well with the observed data in the ferroelectric phase. Damping constant (linewidth) of the SLT crystal was predicted as a function of temperature by using both the pseudospin-phonon coupled and EF models. Our calculated values of the damping constant can be compared with the observed data when they are available in the literature.

The temperature dependence of the inverse relaxation time was calculated below and above the transition temperature of SLT crystal as studied here by using our calculated values of the integrated intensities and calculated values of the damping constant through the PS model and the EF model. The inverse relaxation time calculated through the EF model agrees better with the observed data than that calculated from the PS model near the transition temperature.

The values of the activation energy were extracted at various temperatures of this crystal close to the transition temperature, which are much greater than the $k_B T_C$ value of the SLT crystal. This is an indication that the SLT crystal undergoes an order-disorder phase transition.

Nomenclature

I	– intensity, [–]
k_B	– Boltzmann constant, [eV K ⁻¹]
P	– order parameter, [–]
T	– temperature, [K]
U	– activation energy, [eV]

Greek symbols

Γ	– damping constant, [–]
τ^{-1}	– inverse relaxation time, [s ⁻¹]

Subscripts

C	– Curie
vib	– vibrational

References

- [1] Gvasaliya, S. N. *et al.*, Neutron and Light Scattering Studies of Nearly Stoichiometric Lithium Tantalate, *Ferroelectrics*, 354 (2007), 1, pp. 63-77

- [2] Voronko, Y. K. *et al.*, Raman Scattering Study of Phase Transitions in Lithium Niobate and Tantalite, *Soviet Physics Solid State*, 29 (1987), 5, pp. 1348-1355
- [3] Faubel, M., Schlemmer S., A Variable Temperature Bolometer for Determining Particle Energy and Absolute Flux in Molecular-Beams, *J. Phys.. E. (Sci. Instr.)*, 21 (1988), 1, pp. 75-79
- [4] Kovar, M., *et al.*, Application of Pyroelectric Properties of LiTaO₃ Single Crystal to Microcalorimetric Measurement of the Heat of Adsorption, *Appl. Sur. Sci.*, 74 (1994), 1, pp. 51-59
- [5] Hikita, T., *Ferroelectrics and Related Substances*, Springer-Verlag, Berlin, 2001
- [6] Kratzig, E., Schirmer, O. F., *Photorefractive Materials and Their Applications*, Springer-Verlag, Berlin, 1988
- [7] Hushur, A. *et al.*, Ferroelectric Phase Transition of Stoichiometric Lithium Tantalate Studied by Raman, Brillouin, and Neutron Scattering, *Phys. Rev. B*, 76 (2007), 6, pp. 064104-1-8
- [8] Tezuka, Y. *et al.*, Hyper-Raman and Raman Studies on the Phase Transition of Ferroelectric LiTaO₃, *Phys. Rev. B*, 49 (1994), 14, pp. 9312-9321
- [9] Zhang, M. S., Scott, J. F., Analysis of Quasielastic Light Scattering in LiTaO₃ near T_c, *Phys. Rev. B*, 34 (1986), 3, pp. 1880-1883
- [10] Tomeno, I., Elastic Properties of LiTaO₃, *J. Phys. Soc. Jpn.*, 51 (1982), 9, pp. 2891-2899
- [11] Tomeno, I., Matsumura, S. Dielectric Properties of LiTaO₃, *Phys. Rev. B*, 38 (1988), 1, pp. 606-614
- [12] Johnston, W. D. Jr., Kaminov, I. P., Temperature Dependence of Raman and Rayleigh Scattering in LiNbO₃ and LiTaO₃, *Phys. Rev.*, 168 (1968), 3, pp. 1045-1054
- [13] Servoin, J. L., Gervais, F., Soft Vibrational mode in LiNbO₃ and LiTaO₃, *Solid State Commun.*, 31 (1979), 5, pp. 387-391
- [14] Kojima, S., *et al.*, Dielectric Properties of Ferroelectric Lithium Tantalate Crystals Studied by Terahertz Time-Domain Spectroscopy, *Jpn. J. Appl. Phys.*, 42 (2003), 1, pp. 6238-6241
- [15] Wiederrecht, G. P., *et al.*, Explanation of Anomalous Polariton Dynamics in LiTaO₃. *Phys. Rev. B*, 51 (1995), 2, 916-931
- [16] Timothy, T. F., *et al.*, Heterodyned Impulsive Stimulated Raman Scattering of Phonon-Polaritons in LiTaO₃ and LiNbO₃, *J. Chem. Phys.*, 117 (2002), 6, pp. 2882-2896
- [17] Raptis, C., Assignment and Temperature Dependence of the Raman Modes of LiTaO₃ Studied over the Ferroelectric and Paraelectric Phases, *Phys. Rev. B*, 38 (1988), 14, pp. 10007-10019
- [18] Jayaraman, A., Ballman, A. A., Effect of Pressure on the Raman Modes in LiNbO₃ and LiTaO₃, *J. Appl. Phys.*, 60 (1986), 3, pp. 1208-1210
- [19] Samuelsen, E. J., Grande, A. P., The Ferroelectric Phase Transition in LiTaO₃ Studied by Neutron Scattering, *Z. Phys. B*, 24 (1976), 2, pp. 2017-210
- [20] Abrahams, S. C., *et al.*, Ferroelectric Lithium Tantalate-III. Temperature Dependence of the Structure in the Ferroelectric Phase and the Para-Electric Structure at 940 K, *J. Phys. Chem. Solids*, 34 (1973), 3, pp. 521-532
- [21] Penna, A. F., *et al.*, Debye-Like Diffusive Central Mode Near the Phase Transition in Ferroelectric Lithium Tantalate, *Solid State Commun.*, 19 (1976), 6, pp. 491-494
- [22] Penna, A. F., *et al.*, Anomalous Polariton Dispersion in LiTaO₃ Near T_c. *Solid State Commun.*, 23 (1976), 6, pp. 377-380
- [23] Brout, R., *Phase Transitions*, Benjamin, New York, USA, 1965
- [24] Laulicht, I., The Drastic Temperature Broadening of Hard Mode Raman Lines of Ferroelectric KDP Type Crystals Near T_c, *J. Phys. Chem. Sol.*, 39 (1978), 8, pp. 901-906
- [25] Schaack, G., Winterfeldt, V., Temperature Behaviour of Optical Phonons Near T_c in Triglycine Sulphate and Triglycine Selenate, II. Evidence of Non-Linear Pseudospin-Phonon Interaction, *Ferroelectrics*, 15 (1977), 1, pp. 35-41
- [26] Fahim, M. A., A Detailed IR Study of the Order-Disorder Phase Transition of NaNO₂, *Thermochimica Acta*, 363 (2000), 1-2, pp. 121-127
- [27] Rakov, A. V., The Influence of Intermolecular Interaction on Line Width in the Raman Spectra of Liquids, *Optics and Spectroscopy*, 7 (1959), 1, pp. 128-131
- [28] Bartoli, F. F., Litovitz, T. A., Raman Scattering: Orientational Motions in Liquids, *J. Phys. Chem. Sol.*, 56 (1972), 1, pp. 413-425